Effect of chitinase-3-like protein 1 on glucose metabolism: *In vitro* skeletal muscle and human genetic association study

Running title: Novel role of CHI3L1 in glucose regulation

So-Young Kwak[1,#], Il Hyeok Seo[2,#], InHyeok Chung[1,3], Shin Ae Kim[2], Jung Ok Lee[2], Hye Jeong Lee[2], Sung Eun Kim[3], Jeong Ah Han[2], Min Ju Kang[2], Su Jin Kim[2], Soo Lim[4], Kyoung Min Kim[4], Ji Hyung Chung[5], Eunice Lim[6], Jong-Ik Hwang[7], Hyeon Soo Kim[2,*], Min-Jeong Shin[1,3,*]

[1]Department of Public Health Sciences, BK21 PLUS Program in Embodiment: Health-Society Interaction, Graduate School, Korea University, Seoul 02841, Korea, [2]Department of Anatomy, Korea University College of Medicine, Korea University, Seoul 02841, Korea, [3]School of Biosystems and Biomedical Sciences, College of Health Science, Korea University, Seoul 02841, Korea, [4]Department of Internal Medicine, Seoul National University College of Medicine, Seoul National University Bundang Hospital, Seongnam, South Korea, [5]Department of Biotechnology, College of Life Science, CHA University, Gyeonggi-do 11160, Korea, [6]University of Michigan, Ann Arbor, MI, USA, [7]Departments of Biomedical Sciences, College of Medicine, Korea University, Seoul 02841, Korea

[#]These authors contributed equally to the study, *These authors jointly directed the study

*Corresponding author: **Hyeon Soo Kim**, Department of Anatomy, Korea University College of Medicine, Seoul 02841, Republic of Korea; Tel: 82-2-2286-1151; E-mail address: anatomykim@korea.ac.kr; **Min-Jeong Shin**, Department of Public Health Sciences, BK21PLUS Program in Embodiment: Health-Society Interaction, Graduate School, Korea University, Seoul 02841 Republic of Korea; Tel: 82-2-3290-5643; E-mail address: mjshin@korea.ac.kr

This is the author manuscript accepted for publication and has undergone full peer review but has not been through the copyediting, typesetting, pagination and proofreading process, which may lead to differences between this version and the Version of Record. Please cite this article as doi: 10.1002/FSB2.20907

NONSTANDARD ABBREVIATIONS

ACC	acetyl-CoA carboxylase
AKT	protein kinase B
AMPK	AMP-activated protein kinase
AS160	Akt substrate of 160 kDa
CaMKK	calcium/calmodulin-dependent protein kinase kinase
CHI3L1	chitinase-3-like protein 1
DM	diabetes
DMEM	Dulbecco's modified Eagle's medium
EPS	electrical pulse stimulation
GLUAUC	glucose response area
GLUT4	glucose transporter type 4
GPCR	G-protein-coupled receptor
GTT	glucose tolerance test
HRP	horseradish peroxidase
IGT	impaired glucose tolerance
IL	interleukin
LCL	lymphoblastoid cell lines
MAPK	mitogen-activated protein kinase
NGT	normal glucose tolerance
PAR2	proteinase-activated receptor 2
PBS	phosphate buffered saline
PFA	paraformaldehyde
PI3K	phosphoinositide 3-kinase
PLC	phospholipase C
TNFα	tumor necrosis factor-α

ABSTRACT

We investigated the effect of chitinase-3-like protein 1 (CHI3L1) on glucose metabolism and its underlying mechanisms in skeletal muscle cells, and evaluated whether the observed effects are relevant in humans. CHI3L1 was associated with increased glucose uptake in skeletal muscles in an AMPK-dependent manner, and

with increased intracellular calcium levels via PAR2. The improvement in glucose metabolism observed in an intraperitoneal glucose tolerance test on male C57BL/6J mice supported this association. Inhibition of the CaMKK was associated with suppression of CHI3L1-mediated glucose uptake. Additionally, CHI3L1 was found to influence glucose uptake through the PI3K/AKT pathway. Results suggested that CHI3L1 stimulated the phosphorylation of AS160 and p38 MAPK downstream of AMPK and AKT, and the resultant GLUT4 translocation. In primary myoblast cells, stimulation of AMPK and AKT was observed in response to CHI3L1, underscoring the biological relevance of CHI3L1. CHI3L1 levels were elevated in cells under conditions that mimic exercise *in vitro* and in exercised mice *in vivo*, indicating that CHI3L1 is secreted during muscle contraction. Finally, similar associations between CHI3L1 and metabolic parameters were observed in humans alongside genotype associations between CHI3L1 and diabetes at the population level. CHI3L1 may be a potential therapeutic target for the treatment of diabetes.

Keywords: Chitinase-3-like protein 1, glucose metabolism, AMPK, myokine, glucose uptake

INTRODUCTION

Skeletal muscle has been identified as a secretory organ (1), that produces, expresses, and releases myokines and other cytokines by exercising muscle fibers (2, 3). Myokines consist of muscle-secreted cytokines that communicate with other organs, including adipose tissue, liver, brain, and immune system, in an autocrine, paracrine, or endocrine manner (4), which has been proposed to mediate the beneficial effects of exercise in regulating whole-body metabolism and treating metabolic diseases.

Chitinase 3-like protein 1 (CHI3L1), also known as YKL-40, was originally identified in mouse breast cancer cells (5). It is a secreted heparin- and chitin-binding glycoprotein that lacks chitinase activity (6, 7) and is expressed by many different cell types, including neutrophils, macrophages, osteoclasts, chondrocytes, fibroblasts, vascular smooth muscle cells, endothelial cells, and skeletal muscle cells (8, 9). CHI3L1 expression is regulated by many different pro-inflammatory cytokines, including interleukin 6 (IL-6), IL-13, interferon-γ, IL-1β, and tumor necrosis factor-α (TNFα) (10). While CHI3L1 is predominantly associated with inflammation and tissue remodeling (10), recent evidence suggests that circulating CHI3L1 levels are elevated in patients with metabolic diseases related to insulin resistance, such as type 2 diabetes and obesity (11, 12). However, the molecular mechanisms and activity of CHI3L1 in these processes remain unclear. A recent report classified CHI3L1 as a myokine that acts via auto- and paracrine mechanisms (8, 13), raising questions as to whether

CHI3L1 influences glucose metabolism and which intracellular signaling pathways in skeletal muscle cells might be involved therein.

In the present study, we evaluated CHI3L1 activity during glucose uptake and explored potential underlying mechanisms responsible for its effects. Our results indicate that CHI3L1 stimulates glucose uptake in skeletal muscles via the AMP-activated protein kinase (AMPK) and protein kinase B (AKT) signaling pathways through proteinase-activated receptor 2 (PAR2). We also observed that CHI3L1 levels were elevated under conditions that mimic exercise *in vitro* and in exercised mice *in vivo*. We then investigated whether CHI3L1 regulation of glucose metabolism is transferrable to humans by evaluating the associations among plasma CHI3L1 levels, *CHI3L1* genetic variants, and lymphocytic *CHI3L1* mRNA expression in humans.

MATERIALS AND METHODS

Reagents

Antibodies against the following proteins were used in this study: phospho-AMPKα (Thr^{172}), acetyl-Coa carboxylase (ACC), phospho-ACC (Ser^{79}), and Akt substrate of 160 kDa (AS160) (Millipore-Upstate, Billerica, MA, USA); AMPKα, AKT, phospho-AKT (Ser^{473}), phospho-AS160 (Thr^{642}), and p38 mitogen-activated protein kinase (MAPK) (Cell Signaling Technology, Beverly, MA, USA); phospho-p38 MAPK (Santa Cruz Biotechnology, Dallas, TX, USA); glucose transporter type 4 (GLUT4) and anti-insulin receptor (Abcam, Cambridge, UK); and β-actin (Enogene, New York, NY, USA). Horseradish peroxidase (HRP)-conjugated secondary antibodies were obtained from Enzo Life Sciences (Farmingdale, MA, USA). Compound C and STO-609 were obtained from Calbiochem (San Diego, CA, USA); insulin, LY294002, and thapsigargin were obtained from Sigma-Aldrich (St. Louis, MO, USA); U73122 and SB203580 were obtained from Abcam; and FSLLRY-NH2 was obtained from Tocris (Bristol, UK). CHI3L1 was purchased from Cusabio (Wuhan, Hubei, China). The fluorescent Ca^{2+} indicator Fluo-3 AM was procured from Invitrogen (Leiden, Netherlands).

Plasma membrane fractionation

A plasma membrane protein extraction kit (Abcam, Cambridge, UK) was used to obtain plasma membrane fractions from the cells in accordance with the manufacturer's protocol.

Immunocytochemistry

Cells were fixed with 4% paraformaldehyde (PFA)/phosphate buffered saline (PBS) and permeabilized with 0.2% Triton-X 100. After blocking with 0.2% bovine serum albumin for 30 min, the cells were incubated with anti-GLUT4 antibody at 1:500 dilution for 60 min and then probed with cyanine dye Cy3-labeled secondary antibody (Molecular Probe, Eugene, OR, USA). Stained cells were visualized on a Zeiss confocal microscope.

Immunodetection of Myc-GLUT4

Cell surface expression of Myc-GLUT4 was quantified using an antibody-coupled colorimetric absorbance assay. Following stimulation, myoblasts stably expressing Myc-GLUT4 were incubated with a polyclonal anti-Myc antibody (1:1000) for 60 min, fixed with 4% PFA in PBS for 10 min, and then incubated with HRP-conjugated goat anti-rabbit IgG (1:1000) for 1 h. The cells were washed six times with PBS and incubated in 1 mL of o-phenylenediamine reagent (0.4 mg/mL) for 30 min. Absorbances of the supernatant were measured at 492 nm.

Cell culture

L6 rat myoblast cells were maintained in Dulbecco's modified Eagle's medium (DMEM; Invitrogen) supplemented with 10% fetal bovine serum and 1% antibiotics at 37 °C in a 5% CO_2 atmosphere.

Measurement of 2-deoxy-d(H^3)-glucose uptake

Two days after cells reached confluence, myotube differentiation was induced by incubation in DMEM supplemented with 2% fetal bovine serum for 6–7 days, with a change of media every 2 days. The cells were washed twice with PBS and then starved in serum-free low-glucose DMEM for 3 h. The cells were then incubated with Krebs Ringer bicarbonate (20 mM N-2-hydroxyethylpiperazine-N'-2-ethanesulphonic acid (HEPES) [pH 7.4], 130 mM NaCl, 1.4 mM KCl, 1 mM $CaCl_2$, 1.2 mM $MgSO_4$, and 1.2 mM KH_2PO_4) followed by incubation with test compounds in the same buffer at 37 °C. The uptake assay was initiated by adding 2-deoxy-d(H^3)-glucose to each well and incubating at 37 °C for 15 min. The assay was terminated by washing with ice-cold PBS. The cells were lysed in 10% sodium dodecyl sulfate (SDS) and mixed with a scintillation cocktail to measure radioactivity.

Immunoblotting analysis

Cells in 6-well plates were washed twice with ice-cold PBS and lysed in 70 μL lysis buffer. The samples were sonicated, centrifuged for 20 min, and then heated to 95 °C for 5 min. Supernatants were resolved on 10% SDS-polyacrylamide gels and transferred to nitrocellulose membranes, which were then incubated overnight at 4 °C with primary antibodies. After six washes in tris-buffered saline with 0.1% Tween 20, the membranes were incubated with HRP-conjugated secondary antibodies at room temperature (RT) for 1 h. The blots were washed and visualized by chemiluminescence using an enhanced chemiluminescence Western Blot Detection System (Amersham International PLC, Buckinghamshire, UK).

Small interfering RNA (siRNA) transfection

Transient transfections were performed using Lipofectamine 2000 (Invitrogen) according to the manufacturer's protocol. Briefly, siRNAs targeting AMPKα2 (L-100623-02; Dharmacon, Lafayette, CO, USA) and AKT2 (L-091136-02; Dharmacon) and a non-targeted control siRNA (D-001810-10, Dharmacon) were generated. siRNAs (5 μL) and Lipofectamine 2000 were each diluted with 95 μL of Opti-MEM Reduced-Serum Medium (Invitrogen) and then combined. The resulting mixtures were incubated at RT for 30 min before being added dropwise to culture wells containing 800 μL of Opti-MEM for a final siRNA concentration of 100 nM.

Reverse transcription-polymerase chain reaction (RT-PCR)

RT-PCR was performed at 55 °C for 20 min using a Thermoscript II One-Step RT-PCR Kit (Invitrogen). cDNA amplification was performed using a GeneAmp PCR System 9700 thermocycler (Applied Biosystems, Warrington, UK). Reverse transcriptase was heat-inactivated in the first step of PCR (95 °C for 10 min). The following primers were used for amplification: *CHI3L1*, 5′-ATGTGGACTATGGTGTGGGG-3′ (sense) and 5′-TGAGCGGGAAGTGTACGTTA-3′ (antisense); *ACTB*, 5′-ATTTGGTCGTATTGGGCGCCTGGTCACC-3′ (sense) and 5′-GAAGATGGTGATGGGATTTC-3′ (antisense); *PAR1*, 5′-GGGCAGGGCAGTCTACTTAA-3′ (sense) and 5′-ATGAGCATGATGGAGGCGTA-3′ (antisense); *PAR2*, 5′-CCAGCCTTGAACATCACCAC-3′ (sense) and 5′-ACAAAGGGGTCTATGCAGCT (antisense); *PAR3*, 5′-TGTATGGGCATCAACCGCTA-3′ (sense) and 5′-GGGCAAAGCAGATGGTGAAA-3′ (antisense); and *PAR4*, 5′-GTCTTGCCACTCACGTTTCA-3′ (sense) and 5′-AGGGTCTACGCAGCTGTTAA-3′ (antisense). The amplification steps were as follows: 32 cycles at 95 °C for 15 sec; at 58 °C (*CHI3L1* and *ACTB*), 61 °C (*PAR1*,

PAR3, and *PAR4*) or 55 °C (*PAR2*) for 30 sec; and at 72 °C for 30 sec, followed by 10 min at 72 °C. A 10 μL sample of each reaction was analyzed by agarose gel electrophoresis.

Intracellular calcium measurement using Fluo-3 AM

Cells were loaded with 5 μM Fluo-3 AM and incubated at 37 °C for 30 min. Following washing with medium, DMEM, or calcium-free DMEM (Thermo Fisher Scientific, Waltham, MA, USA) was added to the wells and the cells were observed using a confocal microscope (Zeiss LSM 510 Meta; Zeiss, Oberkochen, Germany) under 200× magnification on a temperature-controlled stage. Excitation and emission wavelengths for signal detection were 488 and 515 nm, respectively.

Primary myoblast preparation

Primary myoblasts were obtained from the forelimbs and hindlimbs of three or four 5-day-old littermate pups. The dissected and minced muscle samples were enzymatically disaggregated in 4 mL of PBS containing 1.5 U/mL dispase II and 1.4 U/mL collagenase D (Roche, Penzberg, Germany) at 37 °C and were triturated with a 10-mL pipette every 5 min for 20 min. The cells were then filtered through a 70-μm mesh (BD Biosciences, Seoul, Korea) and collected by centrifugation at 1,000 rpm for 5 min. The cell pellet was dissolved in 10 mL of F10 medium (Invitrogen) supplemented with 10 ng/mL basic fibroblast growth factor (PeproTech, Princeton, NJ, USA) and 10% cosmic calf serum (Hyclone, Logan, UT, USA). Finally, the cells were pre-plated twice onto non-collagen-coated plates for 1 h each to deplete the fibroblasts. Differentiation was induced by culturing primary myoblasts in DMEM containing antibiotics and 5% horse serum (Invitrogen).

Electrical pulse stimulation (EPS)

To mimic the effect of exercise in *in vitro* model, EPS was applied to cells to induce muscle contraction using a C-Pace EP culture pacer (IonOptix, Westwood, MA, USA), a multi-channel stimulator designed for the chronic stimulation of bulk quantities of cells in culture. This instrument emits bipolar pulses to culture media via immersed carbon electrodes in a C-dish. EPS was applied to L6 cells cultured in high-density micro-mass (2×10^5 cells/mL) conditions under electrical fields of 25 V/cm, with a duration of 5 m/s and a frequency of 1 Hz. At appropriate time points, the cells were harvested either in TRIzol reagent (Invitrogen) for PCR analysis or in lysis buffer for Western blot.

Exercise session and intraperitoneal glucose tolerance test (GTT) in animals

After acclimatization for 1 week, twenty 10-week-old, specific-pathogen-free, male ICR mice (24–28 g; Koatech, Gyeonggido, Korea) were randomly divided into two groups: the control (n = 10) and exercise group (n = 10). Mice in the exercise groups were forced to perform exercise at a 10 m/min velocity for 60 min at a time using a motorized running wheel (20 cm diameter by 5 cm width; Shandong Yiyuan Technology Development Co., Shandong, Binzhou, China) for a day. The mice were sacrificed, and the plasma was collected for ELISA testing (MyBioSource, San Diego, USA). Their quadriceps femoris muscle was further prepared for biochemical analysis. The protocols were approved by the Institutional Animal Care and Use Committee of Korea University (Korea-2016-0252) and were conducted in accordance with the Guide for the Care and Use of Laboratory Animals published by the U.S. National Institutes of Health.We examined the effect of CHI3L1 on glucose metabolism *in vivo* by conducting a metabolic GTT study in a high-fat diet (HFD)-induced obese mouse model. Five-week-old male mice were purchased from Central Lab Animal Inc. (Seoul, Korea) and were maintained in accordance with the guidelines of the Institutional Animal Care and Use Committee of Korea University (KUIACUC-2018-63, KUIACUC-2018-0008). Mice were housed at 18–24 °C with a 12/12 h light/dark cycle, fed HFD ad libitum, and allowed unlimited access to water. A GTT was performed on two randomly assigned groups as a PBS injection (n = 8) or CHI3L1 injection (n = 8). Briefly, mice were fasted overnight (16 h), and a fixed dose of CHI3L1 (5 mg/kg body weight) or PBS followed by glucose (1 g/kg in PBS) was administered. Blood glucose levels were measured in tail vein blood with a glucometer (Accu-Check, Roche, Germany) at 0, 15, 30, 60, 90, and 120 min post-injection.

Association between plasma levels of CHI3L1 and diabetic status in humans

The associations of blood CHI3L1 levels with anthropometric and metabolic parameters in humans were tested using datasets in a clinical setting (n = 80). Plasma levels of CHI3L1 were determined by ELISA immunoassay (CHI3L1 ELISA kit; FineTest). The study participants were divided into four groups based on age and diabetes status as follows: young-normal glucose tolerance (NGT; aged 25–35 years, n = 20), old NGT (aged 65–87 years, n = 20), old-impaired glucose tolerance (IGT; aged 65–88 years, n = 20), and old-diabetes (DM; aged 65–89 years, n = 20). IGT was defined by 2-hour plasma glucose levels 140–199 mg/dL (14), and DM was defined as fasting glucose of at least 126 mg/dL and/or hemoglobin A1c of at least 6.5%, or treatment with antidiabetic medication. All study participants provided written informed consent before starting the experiments. This study was approved by the Institutional Review Board (IRB) of Seoul National University Bundang Hospital (B-1505/298-005) in compliance with the principles of the Declaration of Helsinki and its

amendments.

Genetic association between CHI3L1 and the risk of diabetes in humans

Genetic associations between a genetic variant of CHI3L1 and incidence of DM and related parameters were assessed using the Korean Genome and Epidemiology Study: Ansan and Ansung (KoGES-ASAS) in a community setting. The KoGES-ASAS study is described in detail elsewhere (15). The baseline survey of KoGES-ASAS was initiated in 2001–2002 with a total of 10,030 participants aged 40–69 years from the Ansan and Ansung areas of South Korea, and follow-up studies were performed every two years. Among the 10,030 participants, 7,820 were included in this study after removing 1,190 for whom genotype data was missing, and 1,020 participants diagnosed with DM, cardiovascular disease, or cancer at baseline. Demographic information on the participants, including sex, age, area, education level, smoking, drinking, and physical activity measured by metabolic equivalents were obtained from a questionnaire survey at each follow-up. Following 75 g oral GTT at baseline, plasma glucose levels were measured at 0, 60, and 120 min, and glucose response area (GLUAUC, mg/dL*h) was calculated. New-onset DM was defined by at least one of the following criteria: self-reported doctor-diagnosed DM, fasting glucose level of at least 126 mg/dL, 120 min glucose levels of at least 200 mg/dL, or taking anti-diabetic medication. Detailed information on genotyping was previously reported elsewhere (16). Briefly, genomic DNA was isolated from the peripheral blood of the participants, genotyped on an Affymetrix Genome-Wide Human SNP Array 5.0 (Affymetrix, Inc., Santa Clara, CA, USA), and imputed using the 1000 Genomes Phase I Integrated Release Version 3 as a reference panel. In the present study, rs10399805 (*CHI3L1*), reported to be responsible for most of the genetic effects on CHI3L1 production, was used in the analysis for testing associations thereof with diabetic traits (17, 18). All study participants provided written informed consent before starting the experiments. This study was approved by the IRB of the Korea Centers for Disease Control and Prevention (KBP-2018-039) and the IRB of Korea University (KUIRB-2018-0041-01). Associations between *CHI3L1* mRNA expression level and diabetic traits were assessed by obtaining lymphoblastoid cell lines (LCLs) from 150 individuals from a subgroup of the KoGES-ASAS (KUIRB-2018-0041-01).

For Reverse transcription quantitative PCR, total RNA was extracted from LCLs using the RNeasy Lipid Tissue Mini Kit (Qiagen, Hilden, Germany) according to the manufacturer's protocol. For Reverse transcription, 1μg of total RNA was reverse transcribed using oligo-dT Superscript™ II reverse transcriptase (Invitrogen). Quantitative PCR was performed under the following conditions: 15 min at 95 °C, followed by 40 cycles of 30 sec at 94 °C, 30 sec at 50–60 °C, and 30 sec at 72 °C. The obtained data were analyzed using the comparative cycle threshold (Ct) method and were normalized to glyceraldehyde 3-phosphate dehydrogenase (*GAPDH*). The

primer sequences were as follows: *CHI3L1*, 5'-AATGGCGGTACTGACTTGATG-3' (forward) and 5'-GAAGACTCTCTTGTCTGTCGGA-3' (reverse); and *GAPDH*, 5'-AACTTTGGCATTGTGGAAGG-3' (forward) and 5'-ACACATTGGGGGTAGGAACA-3' (reverse). Lastly, 134 individuals with LCL samples available for experiments were divided into four groups based on *CHI3L1* mRNA expression level (divided by a median, low vs. high) and physical activity (divided by metabolic equivalent median, active vs. inactive) to examine potential mediating effects of physical activity on the association between *CHI3L1* mRNA expression and diabetic traits. The physically active with higher *CHI3L1* mRNA expression group (n = 31) and physically inactive with lower *CHI3L1* mRNA expression (n = 32) group were directly compared.

Statistical analysis

Results for the experiments on cell systems and animals are presented as mean ± standard error of the mean (SEM), and differences among the experimental groups were analyzed using Student's *t*-test or oneway analysis of variance (ANOVA) followed by Bonferroni post-test. Statistical analyses of human studies were performed using the Stata SE 13.0 (Stata, College Station, TX, USA) and GraphPad Prism 5.0 (GraphPad Software, Inc., San Diego, CA, USA) software packages. GLUAUC values were log-transformed to mimic normal distribution. Comparisons of plasma CHI3L1 levels, *CHI3L1* mRNA expression levels, and GLUAUC levels among groups were performed using Student's *t*-test and results are presented as mean ± SEM. The genetic effect of rs10399805 (*CHI3L1*) on the incidence of diabetes and GLUAUC levels were conducted using the Cox proportional hazard regression, and multiple linear regression models, respectively. Genetic associations were examined under a dominant model (GG vs. GA+AA) after adjusting for potential confounders, including sex, age, area, education level, smoking, drinking, hypertension, and metabolic equivalents, and results are presented as hazard ratio (HR) or beta coefficient with 95% confidence intervals (CIs). A *p*-value of less than 0.05 was considered statistically significant.

RESULTS

CHI3L1 stimulates glucose uptake via AMPK in skeletal muscle cells

Skeletal muscle is an important organ for glucose homeostasis because it induces glucose uptake to help maintain normal glucose levels (19). We performed a glucose uptake assay to investigate the role of CHI3L1 in glucose homeostasis, and found that CHI3L1 treatment of L6 cells was associated with time- (Fig. 1A) and dose- (Fig. 1B) dependent increases in glucose uptake. CHI3L1 was shown to induce a greater amount of glucose uptake than insulin, used as a positive control (Fig. 1C). We evaluated the phosphorylation of AMPK, a key molecule involved in glucose uptake, to identify molecular mechanisms through which CHI3L1 affects glucose uptake. CHI3L1 treatment of L6 cells induced phosphorylation of AMPK and its downstream molecule, ACC, in a time- (Fig. 1D) and dose- (Fig. 1E) dependent manner. This effect was blocked by the AMPK inhibitor, Compound C (Fig. 1F). Consistent with this result, the inhibition of AMPK was associated with suppressed CHI3L1-mediated glucose uptake (Fig. 1G). Since compound C potentially inhibits other kinases than AMPK, we then used siRNA to specifically knockdown AMPKα2 expression in L6 cells (Fig.1H) and observed that CHI3L1-induced glucose uptake was blocked by siRNA-mediated knockdown of AMPKα2 (Fig. 1I). These results suggest that CHI3L1 stimulates glucose uptake via AMPK in skeletal muscle cells. In line with these findings, we also observed that intraperitoneal injection of 5 mg/kg CHI3L1 improved glucose metabolism, as measured by GTT and glucose response area (Fig. 1J), in mice.

CHI3L1 stimulates GLUT4 translocation in skeletal muscle cells

GLUT4 is highly expressed in adipose tissue and skeletal muscle, where it facilitates the diffusion of circulating glucose into muscle and fat cells along a concentration gradient (20, 21). GLUT4 translocation is stimulated by insulin or muscle contraction and helps regulate whole-body glucose homeostasis (22). GLUT4 translocation to the plasma membrane was elevated in the presence of CHI3L1, as shown by plasma membrane fractionation (Fig. 2A) and immunocytochemistry (Fig. 2B). Myc-GLUT4 levels in the plasma membrane were increased after CHI3L1 treatment (Fig. 2C) and this effect was suppressed in the presence of Compound C (Fig. 2D). The phosphoinositide 3-kinase (PI3K)/AKT signaling inhibitor LY294002 also suppressed CHI3L1-associated Myc-GLUT4 levels (Fig. 2E). These results suggest that CHI3L1 stimulates GLUT4 translocation to the plasma membrane in skeletal muscle cells.

CHI3L1 increases intracellular Ca^{2+} via PAR2 and activated AMPK pathway

PAR2, also known as GPR11, is a G-protein-coupled receptor (GPCR) that stimulates the release of intracellular calcium, a second messenger frequently employed in signal transduction (23). PAR2 mediates CHI3L1-induced responses in skeletal muscle (8, 13). We measured intracellular calcium levels by staining L6 cells with the calcium-binding dye Fluo-3 AM. CHI3L1 was associated with an increase in fluorescence intensity, an indicator of calcium concentration. We set out to confirm that CHI3L1 increased intracellular calcium levels by measuring fluorescence intensity in the presence of CHI3L1 in a calcium-free medium, and then by depleting the endoplasmic reticulum calcium with thapsigargin, a Ca^{2+}-ATPase inhibitor. Fluorescence intensity increased in the presence of CHI3L1 in calcium-free media but remained unchanged with pretreatment with thapsigargin (Fig. 3A). Many cell surface receptors, including GPCRs, activate phospholipase C (PLC), which stimulates the release of calcium from the endoplasmic reticulum. Treatment with the PLC inhibitor U73122 blocked the induction of AMPK phosphorylation associated with CHI3L1 (Fig. 3B). The presence of U73122 also prevented CHI3L1-associated glucose uptake (Fig. 3C). Calcium/Calmodulin-dependent protein kinase kinase (CaMKK) , an upstream kinase of AMPK, requires calcium as a co-factor to induce AMPK phosphorylation. CaMKK inhibition with STO-609 blocked CHI3L1-associated AMPK phosphorylation (Fig. 3D) and also blocked CHI3L1-associated glucose uptake (Fig. 3E). We then examined the expression patterns of different PARs to identify the specific CHI3L1 receptor involved in glucose homeostasis and found that PAR1, -2, -3, and -4 were all expressed in L6 cells (Fig. 3F). The PAR2 antagonist FSLLRY-NH2 blocked CHI3L1-associated AMPK phosphorylation (Fig. 3G) and also blocked CHI3L1-associated glucose uptake (Fig. 3H). These results indicate that CHI3L1 releases intracellular Ca^{2+} to activate the CaMKK/AMPK pathway via PAR2.

Effect of CHI3L1 on downstream targets of AMPK via AS160 and p38 MAPK pathway

AS160 is a Rab GTPase-activating protein. Phosphorylation of AS160 mediates the translocation of the glucose transporter GLUT4 to the plasma membrane in fat and muscle cells (24) and AS160 acts downstream of AMPK and AKT signaling during glucose uptake (25). CHI3L1 was associated with AS160 phosphorylation in L6 cells in a time- (Fig. 4A) and dose- (Fig. 4B) dependent manner. Inhibition of AMPK blocked the CHI3L1-associated phosphorylation of AS160 (Fig. 4C), as did the siRNA-mediated knockdown of AMPKα2 (Fig. 4D). p38 MAPK functions downstream of AMPK phosphorylation during glucose uptake (26) to regulate GLUT4 activity in skeletal muscle (27). We found that CHI3L1 was associated with p38 MAPK phosphorylation in L6

cells while the knockdown of AMPKα2 by siRNA suppressed CHI3L1-associated p38 MAPK phosphorylation (Fig. 4E). Also, the p38 MAPK inhibitor SB203580 suppressed CHI3L1-associated glucose uptake (Fig. 4F). These results indicate that the p38 MAPK pathway participates in CHI3L1-mediated glucose uptake.

CHI3L1 activates AKT signaling to stimulate glucose uptake

We next explored the role of CHI3L1 in the PI3K/AKT signaling pathway, another key pathway mediating glucose uptake. CHI3L1 was associated with AKT phosphorylation in L6 cells in a time- (Fig. 5A) and dose- (Fig. 5B) dependent manner. The PAR2 antagonist FSLLRY-NH2 blocked this effect (Fig. 5C). The PI3K-specific inhibitor LY294002 blocked CHI3L1-associated AKT phosphorylation (Fig. 5D) and also blocked CHI3L1-associated glucose uptake (Fig. 5E). Inhibition of PI3K/AKT signaling also suppressed CHI3L1-associated AS160 phosphorylation (Fig. 5F), as did the siRNA-mediated knockdown of AKT2 (Fig. 5G). These results suggest that AKT mediates CHI3L1-associated glucose uptake, and CHI3L1 stimulates AS160 phosphorylation via AKT signaling.

CHI3L1 activates AMPK phosphorylation in primary cultured myoblasts

To investigate the effects of CHI3L1 in a biologically relevant system, we used primary cultured myoblasts and found that CHI3L1 was associated with phosphorylation of AMPK and AKT, which increased in a time-dependent manner (Fig. 6A). CHI3L1 was also observed to increased calcium levels in primary myoblasts (Fig. 6B). The inhibition of CaMKK blocked CHI3L1-associated AMPK phosphorylation (Fig. 6C) and the inhibition of AMPK blocked CHI3L1-associated AS160 and p38 MAPK phosphorylation in primary myoblasts (Fig. 6D). These results indicate that CHI3L1 induces AMPK-mediated AS160 phosphorylation alongside AKT activation in primary cultured myoblasts, a biologically relevant effect.

Exercise elevates CHI3L1 expression in skeletal muscle cells

Exercise induces muscle contraction and AMPK activation (28). Muscle contraction alters the muscle secretome of myokines and metabolites that mediates crosstalk between the exercising muscle and distant target organs (29). EPS is used to induce muscle contraction *in vitro* and thereby mimic the effect of exercise (29). *CHI3L1* mRNA expression levels were increased after EPS in a time-dependent manner (Fig. 7A) alongside an increase in AMPK phosphorylation in L6 cells (Fig. 7B). Circulating CHI3L1 levels were also elevated in mice exposed

to exercise (Fig. 7C), and AMPK phosphorylation levels were higher in the muscle tissues of these mice than in controls (Fig. 7D). These results suggest that exercise elevates CHI3L1 expression both *in vitro* and *in vivo*.

Associations among plasma CHI3L1 levels, CHI3L1 genetic variants, and lymphocytic CHI3L1 mRNA expression in humans

We then set out to investigate whether CHI3L1 regulation of glucose metabolism is relevant in humans and thereby assessed potential associations among plasma CHI3L1 levels, *CHI3L1* genetic variants, and lymphocytic *CHI3L1* mRNA expression using two different datasets (clinical and community settings). Data from the clinical setting showed that old age was significantly associated with higher plasma levels of CHI3L1 (young NGT group; 25–35 years; n = 20: 24.1 ± 2.3 ng/mL vs. old NGT group; 65–87 years, n = 20: 143.1 ± 18.1 ng/mL, $p < 0.0001$) (Fig. 8A). Next, we compared plasma CHI3L1 levels according to diabetic status among old participants. Subjects with IGT and DM were grouped together and compared to the NGT group to assess the effect of impaired glucose metabolism. The old IGT + DM group showed significantly lower plasma CHI3L1 levels than those of the old NGT group (80.3 ± 7.6 ng/mL vs. 143.1 ± 18.1 ng/mL, $p = 0.0004$) (Fig. 8B). Regarding the risk of DM in a community setting via the KoGES-ASAS study, the presence of the minor allele of rs10399805 (*CHI3L1*) was associated with a 15% lower risk of DM (HR: 0.85, 95% CI: 0.73 to 0.98, $p = 0.023$) (Fig. 8C), and 2.9-fold greater *CHI3L1* mRNA expression in LCLs ($p = 0.0048$) (Fig. 8D). We also observed that rs10399805 was associated with lower GLUAUC levels (beta coefficient: -0.005, 95% CI: -0.009 to -0.000, $p = 0.039$) (Fig. 8C). Finally, we tested whether *CHI3L1* mRNA expression is associated with GLUAUC in a subset of KoGES-ASAS study participants (n = 134). No significant association between *CHI3L1* mRNA expression in LCLs and GLUAUC was observed. However, physical activity modified this association, as physically active participants with higher *CHI3L1* mRNA expression levels presented lower GLUAUC levels than physically inactive individuals with lower *CHI3L1* mRNA expression levels (268.8 ± 8.5 vs. 242.1 ± 8.6 mg/dL*h, $p = 0.0308$) (Fig. 8E).

DISCUSSION

Several studies have reported that CHI3L1 is associated with a range of inflammatory diseases, including asthma and autoimmune pathologies (30, 31). However, potential biological functions of CHI3L1 and its underlying molecular mechanisms in metabolic conditions remain unclear. In the present study, we hypothesized that CHI3L1 regulates glucose metabolism by activating multiple intracellular signaling pathway (Fig. 9). Our results indicate that CHI3L1 stimulated glucose uptake via AMPK in skeletal muscle cells as well as in primary cultured myoblasts; this was further supported by improved GTT following CHI3L1 injection in mice. Also, CHI3L1 was shown to induce p38 MAPK phosphorylation in L6 cells, an effect that was blocked by AMPK knockdown. p38 MAPK functions downstream of AMPK phosphorylation during glucose uptake (26). Based on the profound influence of the AMPK signaling pathway on glucose metabolism (32), we first assessed levels of AMPK pathway-associated proteins to uncover the underlying mechanisms involved in the influence of CHI3L1 on glucose uptake in skeletal muscle cells. AMPK is a heterotrimeric complex consisting of a catalytic subunit (α) and two regulatory subunits (β and γ) and is critical to growth regulation, cellular processes, and metabolism reprogramming (33). AMPK is activated by an increase in the AMP–ATP ratio in response to cellular stress, such as that exerted by skeletal muscles (34) during exercise. CaMKK, which responds to calcium flux, and liver kinase B1, which exists in a heterotrimeric complex with STRAD and MO25, have been identified as upstream kinases of AMPK (35-38). Glucose uptake, necessary for the maintenance of whole-body glucose homeostasis, involves the delivery of glucose to adipose tissue and skeletal muscle via glucose transporters (19). AMPK also participates in glucose uptake independent of insulin signaling (39). AMPK activation is induced by changes in cellular energy status, such as muscle contraction (40). In the present study, we found that CHI3L1 stimulated glucose uptake and GLUT4 translocation in an AMPK-dependent manner in skeletal muscle cells. Our results indicate that CHI3L1 is secreted as a result of muscle contraction to increase glucose uptake via translocation of GLUT4 through the AMPK signaling pathway.

Along with the AMPK pathway and downstream p38 MAPK pathway, our results showed the AKT pathway was also involved in mediating CHI3L1-associated glucose uptake and GLUT4 translocation, as evidenced by phosphorylation of AS160. AKT is a serine/threonine-specific protein kinase that is an important signaling molecule in glucose homeostasis (41). We observed that PAR2, also called GPR11, is directly involved in CHI3L1-associated intracellular Ca^{2+} release and participates in downstream activation of the CaMKK/AMPK pathway in skeletal muscles. IL-13Rα2 (42) and PAR2 (8, 13) have recently been identified as CHI3L1-specific

receptors, with PAR2 as the primary CHI3L1 receptor in skeletal muscle (8, 13). In the present study, we demonstrated that PAR2 mediated CHI3L1-associated glucose homeostasis and that PAR1, -3, and -4 might also act as CHI3L1 receptors. The PAR2 receptor has been identified in almost all human organs (43), and CHI3L1 may thus be capable of influencing biological processes in almost all tissues, which inhibits its potential as a therapeutic drug. Our results are in line with previous findings that CHI3L1 treatment blocked TNFα-induced inflammation by inhibiting nuclear factor κB activation in skeletal muscle cells, a process that is mediated by PAR2 (13). Treatment of CHI3L1 in cultured human myoblasts was reported to stimulate the activation of p44/42, p38 MAPK, and AKT and enhance myoblast proliferation (8). Meanwhile, there is also possible involvement of other PAR dependent or even independent signaling pathways since PAR2 antagonizing was not enough to fully attenuate the function of CHI3L1. Taken together, our findings indicate that CHI3L1 can enhance glucose uptake and GLUT4 translocation by stimulating AMPK and AKT pathways in skeletal muscle *in vitro*. This was supported by *in vivo* results in mice, which showed that CHI3L1 was secreted from muscle tissue into the bloodstream after exercise. We thereby surmise that CHI3L1 is a myokine that regulates glucose metabolism.

We further tested the hypothesis that the observed effects of CHI3L1 on glucose metabolism is relevant to humans. Accumulating studies have consistently reported that circulating levels of CHI3L1 are elevated in inflammatory diseases and related pathological conditions, such as asthma (30), atopy (17), and rheumatoid arthritis (18), suggesting it is a biomarker for inflammation. Conversely, reports on the association of blood CHI3L1 levels with metabolic conditions remain inconclusive. A few studies have shown that plasma levels of CHI3L1 are increased in obesity, insulin resistance, and type 2 diabetes (11, 12); however, no insulin sensitivity indexes were found to be significantly associated with plasma CHI3L1 levels in a Danish sample (44), suggesting that CHI3L1 is not directly involved in the development of type 2 diabetes. Besides, plasma CHI3L1 level was not associated with insulin resistance in a human study using hyperinsulinemic-euglycemic clamp (45). A study by Park et al (46) conducted in Koreans showed higher CHI3L1 levels in diabetic patients compared to non-diabetic control, however, the very small sample size (only four diabetic patients for comparison) limits the generalization of the results. In contrast to previous findings (11, 12, 46), our results showed that the plasma levels of CHI3L1 were significantly lower in old participants with impaired glucose metabolism than those in normal control. CHI3L1 has been proposed to be an auto-protective factor that is induced upon demand to protect skeletal muscle cells from the negative impact of TNFα, suggesting that CHI3L1 is a rescue myokine that is produced on demand such as inflammatory responses (13). Thus, it can be

speculated that circulating levels of CHI3L1 may increase during low grade inflammation such as obesity and insulin resistance, but decrease progressively to reverse the metabolic derangement in type 2 diabetes. Alternatively, the ethnic background of the study population could partially explain this discrepancy. As a matter of fact, previous studies have shown that the genetic variants affecting CHI3L1 levels are inconsistent between ethnic groups (17, 47). The reduced CHI3L1 in type 2 diabetes shown in this study was further supported by a genetic association study on a Korean population. A genetic variant of *CHI3L1* (rs10399805) located at its promoter region has been reported to increase the production of CHI3L1 in different populations (17, 18). A functional study conducted on Koreans reported that the genetic variant at *CHI3L1* (rs10399805) was associated with significantly higher serum CHI3L1 levels, a 2.5-fold increase in *CHI3L1* mRNA expression in peripheral blood cells, and increased risk of atopy in Koreans (17). In this study, a targeted genetic association study showed that the minor allele of rs10399805 (*CHI3L1*) was associated with higher *CHI3L1* mRNA expression in LCLs together with lower levels of glucose response area, supporting the hypothesis that plasma levels of CHI3L1 are reduced in type 2 diabetics in this population. Of note, our results also showed that physical activity synergistically interacts with *CHI3L1* expression to mediate glucose responses in humans. Finally, our longitudinal genetic study revealed that the minor allele of rs10399805 (*CHI3L1*) was associated with a significantly lower risk for DM. Our results, together with those showing protective effects of CHI3L1 on TNFα-induced insulin resistance and inflammation *in vitro* (13) led us to speculate that reduced levels of plasma CHI3L1 are associated with aberrant glucose metabolism in humans, which requires further confirmation in a larger and more diverse population.

In conclusion, our results indicate that CHI3L1 is a myokine that stimulates glucose uptake in skeletal muscles via the AMPK and AKT signaling pathways through PAR2, which is further relevant in glucose metabolism of humans. Further studies are needed to elucidate the biological functions of CHI3L1 and to better understand the relationship between CHI3L1 and glucose metabolism. Our results suggest CHI3L1 as a novel candidate for therapeutics for human diabetes and related metabolic diseases.

ACKNOWLEDGEMENT

This study was conducted with bioresources from National Biobank of Korea, the Centers for Disease Control and Prevention, Republic of Korea (KBP-2018-039). This study was supported by the National Research Foundation of Korea (NRF), which is funded by the Korean government (NRF-2016R1A2B4014418). This study was also supported by the Basic Science Research Program through the NRF funded by the Ministry of Science and ICT (NRF-2020R1A2C2005580) and by the Bio & Medical Technology Development Program of the NRF funded by the Ministry of Science & ICT (NRF-2012M3A9C4048761). The authors confirm that there are no conflicts of interest.

AUTHOR CONTRIBUTIONS

H.S.K. and M.J.S conceived the study and designed and directed the project. S.Y.K., I.S., I.C., S.A.K., J.O.L., H.J.L., J.A.H., M.J.K., and S.J.K. performed experiments and acquired the data. S.Y.K., I.S., I.C., H.S.K., and M.J.S. analyzed and interpreted the results. S.E.K. and J.I.H reviewed/edited the manuscript and contributed to the discussion. S.L. and K.M.K. directed and conducted the human clinical study. S.Y.K., I.S., J.H.C., E.L., H.S.K., and M.J.S. wrote the manuscript and contributed to the discussion. All authors approved the submission of the article.

REFERENCES

1. Pedersen, B. K., Akerstrom, T. C., Nielsen, A. R., and Fischer, C. P. (2007) Role of myokines in exercise and metabolism. *J Appl Physiol (1985)* **103**, 1093-1098
2. Pedersen, B. K., and Febbraio, M. A. (2012) Muscles, exercise and obesity: skeletal muscle as a secretory organ. *Nat Rev Endocrinol* **8**, 457-465
3. Pedersen, B. K., Steensberg, A., Fischer, C., Keller, C., Keller, P., Plomgaard, P., Febbraio, M., and Saltin, B. (2003) Searching for the exercise factor: is IL-6 a candidate? *J Muscle Res Cell Motil* **24**, 113-119
4. Pedersen, B. K., and Febbraio, M. A. (2008) Muscle as an endocrine organ: focus on muscle-derived interleukin-6. *Physiol Rev* **88**, 1379-1406
5. Morrison, B. W., and Leder, P. (1994) neu and ras initiate murine mammary tumors that share genetic markers generally absent in c-myc and int-2-initiated tumors. *Oncogene* **9**, 3417-3426
6. Renkema, G. H., Boot, R. G., Au, F. L., Donker-Koopman, W. E., Strijland, A., Muijsers, A. O.,

Hrebicek, M., and Aerts, J. M. (1998) Chitotriosidase, a chitinase, and the 39-kDa human cartilage glycoprotein, a chitin-binding lectin, are homologues of family 18 glycosyl hydrolases secreted by human macrophages. *Eur J Biochem* **251**, 504-509

7. Shao, R., Hamel, K., Petersen, L., Cao, Q. J., Arenas, R. B., Bigelow, C., Bentley, B., and Yan, W. (2009) YKL-40, a secreted glycoprotein, promotes tumor angiogenesis. *Oncogene* **28**, 4456-4468
8. Gorgens, S. W., Hjorth, M., Eckardt, K., Wichert, S., Norheim, F., Holen, T., Lee, S., Langleite, T., Birkeland, K. I., Stadheim, H. K., Kolnes, K. J., Tangen, D. S., Kolnes, A. J., Jensen, J., Drevon, C. A., and Eckel, J. (2016) The exercise-regulated myokine chitinase-3-like protein 1 stimulates human myocyte proliferation. *Acta Physiol (Oxf)* **216**, 330-345
9. Di Rosa, M., and Malaguarnera, L. (2016) Chitinase 3 Like-1: An Emerging Molecule Involved in Diabetes and Diabetic Complications. *Pathobiology* **83**, 228-242
10. Lee, C. G., Da Silva, C. A., Dela Cruz, C. S., Ahangari, F., Ma, B., Kang, M. J., He, C. H., Takyar, S., and Elias, J. A. (2011) Role of chitin and chitinase/chitinase-like proteins in inflammation, tissue remodeling, and injury. *Annu Rev Physiol* **73**, 479-501
11. Rathcke, C. N., Johansen, J. S., and Vestergaard, H. (2006) YKL-40, a biomarker of inflammation, is elevated in patients with type 2 diabetes and is related to insulin resistance. *Inflamm Res* **55**, 53-59
12. Kyrgios, I., Galli-Tsinopoulou, A., Stylianou, C., Papakonstantinou, E., Arvanitidou, M., and Haidich, A. B. (2012) Elevated circulating levels of the serum acute-phase protein YKL-40 (chitinase 3-like protein 1) are a marker of obesity and insulin resistance in prepubertal children. *Metabolism* **61**, 562-568
13. Gorgens, S. W., Eckardt, K., Elsen, M., Tennagels, N., and Eckel, J. (2014) Chitinase-3-like protein 1 protects skeletal muscle from TNFalpha-induced inflammation and insulin resistance. *Biochem J* **459**, 479-488
14. Nathan, D. M., Davidson, M. B., DeFronzo, R. A., Heine, R. J., Henry, R. R., Pratley, R., and Zinman, B. (2007) Impaired fasting glucose and impaired glucose tolerance: implications for care. *Diabetes Care* **30**, 753-759
15. Kim, Y., Han, B.-G., and Ko, G. E. S. g. (2017) Cohort Profile: The Korean Genome and Epidemiology Study (KoGES) Consortium. *Int J Epidemiol* **46**, e20
16. Cho, Y. S., Go, M. J., Kim, Y. J., Heo, J. Y., Oh, J. H., Ban, H.-J., Yoon, D., Lee, M. H., Kim, D.-J., Park, M., Cha, S.-H., Kim, J.-W., Han, B.-G., Min, H., Ahn, Y., Park, M. S., Han, H. R., Jang, H.-Y., Cho, E. Y., Lee, J.-E., Cho, N. H., Shin, C., Park, T., Park, J. W., Lee, J.-K., Cardon, L., Clarke, G., McCarthy, M. I., Lee, J.-Y., Lee, J.-K., Oh, B., and Kim, H.-L. (2009) A large-scale genome-wide association study of Asian populations uncovers genetic factors influencing eight quantitative traits. *Nat*

Genet **41**, 527-534

17. Sohn, M. H., Lee, J. H., Kim, K. W., Kim, S. W., Lee, S. H., Kim, K.-E., Kim, K. H., Lee, C. G., Elias, J. A., and Lee, M. G. (2009) Genetic variation in the promoter region of chitinase 3-like 1 is associated with atopy. *Am J Respir Crit Care Med* **179**, 449-456
18. Nielsen, K. R., Steffensen, R., Boegsted, M., Baech, J., Lundbye-Christensen, S., Hetland, M. L., Krintel, S. B., Johnsen, H. E., Nyegaard, M., and Johansen, J. S. (2011) Promoter polymorphisms in the chitinase 3-like 1 gene influence the serum concentration of YKL-40 in Danish patients with rheumatoid arthritis and in healthy subjects. *Arthritis Res Ther* **13**, R109
19. Leney, S. E., and Tavare, J. M. (2009) The molecular basis of insulin-stimulated glucose uptake: signalling, trafficking and potential drug targets. *J Endocrinol* **203**, 1-18
20. Richter, E. A., and Hargreaves, M. (2013) Exercise, GLUT4, and skeletal muscle glucose uptake. *Physiol Rev* **93**, 993-1017
21. Watson, R. T., Kanzaki, M., and Pessin, J. E. (2004) Regulated membrane trafficking of the insulin-responsive glucose transporter 4 in adipocytes. *Endocr Rev* **25**, 177-204
22. Huang, S., and Czech, M. P. (2007) The GLUT4 glucose transporter. *Cell Metab* **5**, 237-252
23. Jairaman, A., Yamashita, M., Schleimer, R. P., and Prakriya, M. (2015) Store-Operated Ca2+ Release-Activated Ca2+ Channels Regulate PAR2-Activated Ca2+ Signaling and Cytokine Production in Airway Epithelial Cells. *J Immunol* **195**, 2122-2133
24. Miinea, C. P., Sano, H., Kane, S., Sano, E., Fukuda, M., Peranen, J., Lane, W. S., and Lienhard, G. E. (2005) AS160, the Akt substrate regulating GLUT4 translocation, has a functional Rab GTPase-activating protein domain. *Biochem J* **391**, 87-93
25. Kramer, H. F., Witczak, C. A., Fujii, N., Jessen, N., Taylor, E. B., Arnolds, D. E., Sakamoto, K., Hirshman, M. F., and Goodyear, L. J. (2006) Distinct signals regulate AS160 phosphorylation in response to insulin, AICAR, and contraction in mouse skeletal muscle. *Diabetes* **55**, 2067-2076
26. Xi, X., Han, J., and Zhang, J. Z. (2001) Stimulation of glucose transport by AMP-activated protein kinase via activation of p38 mitogen-activated protein kinase. *J Biol Chem* **276**, 41029-41034
27. Niu, W., Huang, C., Nawaz, Z., Levy, M., Somwar, R., Li, D., Bilan, P. J., and Klip, A. (2003) Maturation of the regulation of GLUT4 activity by p38 MAPK during L6 cell myogenesis. *J Biol Chem* **278**, 17953-17962
28. Richter, E. A., and Ruderman, N. B. (2009) AMPK and the biochemistry of exercise: implications for human health and disease. *Biochem J* **418**, 261-275
29. Evers-van Gogh, I. J., Alex, S., Stienstra, R., Brenkman, A. B., Kersten, S., and Kalkhoven, E. (2015)

Electric Pulse Stimulation of Myotubes as an In Vitro Exercise Model: Cell-Mediated and Non-Cell-Mediated Effects. *Sci Rep* **5**, 10944

30. Chupp, G. L., Lee, C. G., Jarjour, N., Shim, Y. M., Holm, C. T., He, S., Dziura, J. D., Reed, J., Coyle, A. J., Kiener, P., Cullen, M., Grandsaigne, M., Dombret, M. C., Aubier, M., Pretolani, M., and Elias, J. A. (2007) A chitinase-like protein in the lung and circulation of patients with severe asthma. *N Engl J Med* **357**, 2016-2027
31. Johansen, J. S. (2006) Studies on serum YKL-40 as a biomarker in diseases with inflammation, tissue remodelling, fibroses and cancer. *Dan Med Bull* **53**, 172-209
32. Herzig, S., and Shaw, R. J. (2018) AMPK: guardian of metabolism and mitochondrial homeostasis. *Nat Rev Mol Cell Biol* **19**, 121-135
33. Mihaylova, M. M., and Shaw, R. J. (2011) The AMPK signalling pathway coordinates cell growth, autophagy and metabolism. *Nat Cell Biol* **13**, 1016-1023
34. Wang, W., Yang, X., Lopez de Silanes, I., Carling, D., and Gorospe, M. (2003) Increased AMP:ATP ratio and AMP-activated protein kinase activity during cellular senescence linked to reduced HuR function. *J Biol Chem* **278**, 27016-27023
35. Hawley, S. A., Pan, D. A., Mustard, K. J., Ross, L., Bain, J., Edelman, A. M., Frenguelli, B. G., and Hardie, D. G. (2005) Calmodulin-dependent protein kinase kinase-beta is an alternative upstream kinase for AMP-activated protein kinase. *Cell Metab* **2**, 9-19
36. Woods, A., Dickerson, K., Heath, R., Hong, S. P., Momcilovic, M., Johnstone, S. R., Carlson, M., and Carling, D. (2005) Ca2+/calmodulin-dependent protein kinase kinase-beta acts upstream of AMP-activated protein kinase in mammalian cells. *Cell Metab* **2**, 21-33
37. Sakamoto, K., McCarthy, A., Smith, D., Green, K. A., Grahame Hardie, D., Ashworth, A., and Alessi, D. R. (2005) Deficiency of LKB1 in skeletal muscle prevents AMPK activation and glucose uptake during contraction. *Embo j* **24**, 1810-1820
38. Koh, H. J., Arnolds, D. E., Fujii, N., Tran, T. T., Rogers, M. J., Jessen, N., Li, Y., Liew, C. W., Ho, R. C., Hirshman, M. F., Kulkarni, R. N., Kahn, C. R., and Goodyear, L. J. (2006) Skeletal muscle-selective knockout of LKB1 increases insulin sensitivity, improves glucose homeostasis, and decreases TRB3. *Mol Cell Biol* **26**, 8217-8227
39. Musi, N., and Goodyear, L. J. (2003) AMP-activated protein kinase and muscle glucose uptake. *Acta Physiol Scand* **178**, 337-345
40. Hayashi, T., Hirshman, M. F., Kurth, E. J., Winder, W. W., and Goodyear, L. J. (1998) Evidence for 5' AMP-activated protein kinase mediation of the effect of muscle contraction on glucose transport.

Diabetes **47**, 1369-1373

41. Leto, D., and Saltiel, A. R. (2012) Regulation of glucose transport by insulin: traffic control of GLUT4. *Nat Rev Mol Cell Biol* **13**, 383-396
42. He, C. H., Lee, C. G., Dela Cruz, C. S., Lee, C. M., Zhou, Y., Ahangari, F., Ma, B., Herzog, E. L., Rosenberg, S. A., Li, Y., Nour, A. M., Parikh, C. R., Schmidt, I., Modis, Y., Cantley, L., and Elias, J. A. (2013) Chitinase 3-like 1 regulates cellular and tissue responses via IL-13 receptor alpha2. *Cell Rep* **4**, 830-841
43. Cicala, C. (2002) Protease activated receptor 2 and the cardiovascular system. *Br J Pharmacol* **135**, 14-20
44. Thomsen, S. B., Gjesing, A. P., Rathcke, C. N., Ekstrom, C. T., Eiberg, H., Hansen, T., Pedersen, O., and Vestergaard, H. (2015) Associations of the Inflammatory Marker YKL-40 with Measures of Obesity and Dyslipidaemia in Individuals at High Risk of Type 2 Diabetes. *PLoS One* **10**, e0133672
45. Toloza, F. J. K., Perez-Matos, M. C., Ricardo-Silgado, M. L., Morales-Alvarez, M. C., Mantilla-Rivas, J. O., Pinzon-Cortes, J. A., Perez-Mayorga, M., Arevalo-Garcia, M. L., Tolosa-Gonzalez, G., and Mendivil, C. O. (2017) Comparison of plasma pigment epithelium-derived factor (PEDF), retinol binding protein 4 (RBP-4), chitinase-3-like protein 1 (YKL-40) and brain-derived neurotrophic factor (BDNF) for the identification of insulin resistance. *J Diabetes Complications* **31**, 1423-1429
46. Park, H. Y., Jun, C. D., Jeon, S. J., Choi, S. S., Kim, H. R., Choi, D. B., Kwak, S., Lee, H. S., Cheong, J. S., So, H. S., Lee, Y. J., and Park, D. S. (2012) Serum YKL-40 levels correlate with infarct volume, stroke severity, and functional outcome in acute ischemic stroke patients. *PLoS One* **7**, e51722
47. Schultz, N. A., and Johansen, J. S. (2010) YKL-40-A Protein in the Field of Translational Medicine: A Role as a Biomarker in Cancer Patients? *Cancers (Basel)* **2**, 1453-1491

FIGURE LEGENDS

Figure 1. CHI3L1 stimulates glucose uptake via AMPK in skeletal muscle cells. (A) L6 myotube cells were incubated with CHI3L1 (100 ng/mL) for the indicated times, followed by glucose uptake assay. (B) L6 myotube cells were incubated with different concentrations of CHI3L1 for 1 h, followed by glucose uptake assay. (C) L6 myotube cells were incubated with CHI3L1 (100 ng/mL) for 1 h or insulin (100 nM) for 15 min, followed by glucose uptake assay. (D) L6 cells were incubated with CHI3L1 (100 ng/mL) for the indicated times. Cell lysates were analyzed by Western blot using antibodies against phospho-AMPKα (Thr^{172}) and phospho-ACC (Ser^{79}). (E) L6 cells were stimulated for 1 h with different concentrations of CHI3L1. Cell lysates were analyzed by Western blot using antibodies against phospho-AMPKα (Thr^{172}) and phospho-ACC (Ser^{78}). (D,E) p-AMPKα and p-ACC levels were quantified by densitometry and normalized to total AMPKα and ACC protein levels. (F) L6 cells were pretreated with the AMPK inhibitor compound C (30 μM) and then with CHI3L1 (100 ng/mL). Cell lysates were analyzed by Western blot using an antibody against phospho-AMPKα (Thr^{172}). AMPKα served as a control. (G) L6 myotube cells were treated with CHI3L1 (100 ng/mL) for 1 h in the presence of compound C (30 μM), followed by glucose uptake assay. (H) L6 cells were transiently transfected with an *AMPKα2* siRNA or a non-target siRNA for 48 h. Cell lysates were analyzed by Western blot using an antibody against AMPKα. β-actin served as a control. (I) L6 cells were transiently transfected with an *AMPKα2* siRNA and non-target siRNA for 48 h. Differentiated cells were incubated with CHI3L1 (100 ng/mL) for 1 h, followed by glucose uptake assay. (A-E,G,I) Data are expressed as means ± standard errors of the means (n = 3), and one-way ANOVA followed by Bonferroni post-test were used to compare between multiple groups. * $p < 0.05$, ** $p < 0.01$ as indicated. (J) Blood glucose levels and glucose response area during GTT in mice on high fat diet injected with either PBS (n = 8) or CHI3L1 (n = 8). Data are expressed as means ± standard errors of the means, and one-way ANOVA followed by Bonferroni post-test were used to compare between multiple groups. * $p < 0.05$, ** $p < 0.01$ as indicated.

Figure 2. CHI3L1 stimulates GLUT4 translocation in skeletal muscle cells. (A) Fractionated plasma membranes from L6 cells were pretreated with CHI3L1 (100 ng/mL) or insulin (100 nM). Plasma membrane proteins were analyzed by Western blot using an antibody against GLUT4. The insulin receptor served as a plasma membrane marker and β-actin as a cytosolic marker. (B) Representative

images (GLUT4, DAPI, and merge) of GLUT4-expressing cells treated with CHI3L1 for 1 h. Insulin (100 nM) was used as a positive control. Scale bars, 10 μm. (C) Confluent monolayers of L6 cells expressing Myc-GLUT4 were incubated with CHI3L1 (100 ng/mL) for 1 h. Cell surface expression of Myc-GLUT4 was detected using an antibody-coupled colorimetric absorbance assay. (D) L6 cells expressing Myc-GLUT4 were pretreated with compound C (30 μM) for 30 min and then incubated with CHI3L1 (100 ng/mL) for 1 h before assessing GLUT4 translocation. (E) L6 cells expressing Myc-GLUT4 were pretreated with LY294002 (20 μM) for 30 min and then incubated with CHI3L1 (100 ng/mL) for 1 h before assessing GLUT4 translocation. (C-E) Data are expressed as means ± standard errors of the means (n = 3), and one-way ANOVA followed by Bonferroni post-test were used to compare between multiple groups. * $p < 0.05$, ** $p < 0.01$ as indicated.

Figure 3. CHI3L1 increases intracellular Ca^{2+} and activates the AMPK pathway via PAR2. (A) L6 cells were preincubated with Fluo-3 AM (5 μM) for 30 min, and intracellular Ca^{2+} response was then measured using a confocal microscope after changing to calcium-free media and treating with CHI3L1. Alternatively, L6 cells were pretreated with the endoplasmic reticulum Ca^{2+}-ATPase inhibitor thapsigargin (1 μM) and Ca^{2+} response was measured using a confocal microscope after treatment with CHI3L1. Scale bars, 100 μm. (B) L6 cells were pretreated with the PLC inhibitor U73122 (10 μM) and then with CHI3L1 (100 ng/mL). Cell lysates were analyzed by Western blot using an antibody against phospho-AMPKα (Thr^{172}). AMPKα served as a control. (C) L6 myotube cells were treated with CHI3L1 (100 ng/mL) for 1 h in the presence of U73122 (10 μM), followed by glucose uptake assay. (D) L6 cells were pretreated with the CaMKK inhibitor STO-609 (5 μM) and then with CHI3L1 (100 ng/mL). Cell lysates were analyzed by Western blot using an antibody against phospho-AMPKα (Thr^{172}). AMPKα served as a control. (E) L6 myotube cells were treated with CHI3L1 (100 ng/mL) for 1 h in the presence of STO-609 (5 μM), followed by glucose uptake assay. (F) Total mRNA was prepared from L6 cells and RT-PCR was performed using specific primers against the PAR family members PAR1, -2, -3, and -4. PCR products were separated on 1.7% agarose gels and visualized under ultraviolet light with *ACTB* as a positive control. (G) L6 cells were pretreated with the selective PAR2 antagonist FSLLRY-NH2 (10 μM) and then with CHI3L1 (100 ng/mL). Cell lysates were analyzed by Western blot using an antibody against phospho-AMPKα (Thr^{172}). AMPKα served as a control. (H) L6 myotube cells were treated with CHI3L1 (100 ng/mL) for 1 h in the presence of FSLLRY-NH2 (10 μM), followed by glucose uptake assay. (C,E,H) Data are expressed as means ± standard errors of the means (n = 3), and one-way

ANOVA followed by Bonferroni post-test were used to compare between multiple groups. * $p < 0.05$, ** $p < 0.01$, *** $p < 0.001$ as indicated.

Figure 4. Effect of CHI3L1 on downstream targets of AMPK via AS160 and p38 MAPK pathway. (A) L6 cells were incubated with CHI3L1 (100 ng/mL) for the indicated times. Cell lysates were analyzed by Western blot using an antibody against phospho-AS160 (Thr^{642}). (B) L6 cells were stimulated with different concentrations of CHI3L1 for 1 h. Cell lysates were analyzed by Western blot using an antibody against phospho-AS160 (Thr^{642}). (A,B) p-AS160 levels were quantified by densitometry and normalized to total AS160 protein levels. (C) L6 cells were pretreated with compound C (30 μM) and then incubated with CHI3L1 (100 ng/mL). Cell lysates were analyzed by Western blot using an antibody against phospho-AS160 (Thr^{642}). AS160 served as a control. (D) L6 cells were transiently transfected with an *AMPKα2* siRNA for 48 h. Cell lysates were analyzed by Western blot using an antibody against phospho-AS160 (Thr^{642}). AS160 served as a control. (E) L6 cells were transiently transfected with an *AMPKα2* siRNA for 48 h. Cell lysates were analyzed by Western blot using an antibody against phospho-p38 MAPK. p38 MAPK served as a control. (F) L6 myotube cells were treated with CHI3L1 (100 ng/mL) for 1 h in the presence of the p38 MAPK inhibitor SB203580 (10 μM), followed by glucose uptake assay. (A,B,F) Data are expressed as means ± standard errors of the means (n = 3), and one-way ANOVA followed by Bonferroni post-test were used to compare between multiple groups. * $p < 0.05$, ** $p < 0.01$, *** $p < 0.001$ as indicated.

Figure 5. CHI3L1 activates AKT signaling to stimulate glucose uptake. (A) L6 cells were incubated with CHI3L1 (100 ng/mL) for the indicated times. Cell lysates were analyzed by Western blot using an antibody against phospho-AKT (Ser^{473}). (B) L6 cells were stimulated for 1 h with different concentrations of CHI3L1. Cell lysates were analyzed by Western blot using an antibody against phospho-AKT (Ser^{473}). (A,B) p-AKT levels were quantified by densitometry and normalized to total AKT protein levels. (C) L6 cells were pretreated with the selective PAR2 antagonist FSLLRY-NH2 (10 μM) and then with CHI3L1 (100 ng/mL). Cell lysates were analyzed by Western blot using an antibody against phospho-AKT (Ser^{473}). AKT served as a control. (D) L6 cells were pretreated with the PI3K inhibitor LY294002 (20 μM) and then with CHI3L1 (100 ng/mL). Cell lysates were analyzed by Western blot using an antibody against phospho-AKT (Ser^{473}). AKT served as a control. (E) L6 myotube cells were treated with CHI3L1 (100 ng/mL) for 1 h in the presence of LY294002 (20 μM), followed by glucose uptake assay. (F) L6 cells were pretreated with LY294002 (20 μM) and then with

CHI3L1 (100 ng/mL). Cell lysates were analyzed by Western blot using an antibody against phospho-AS160 (Thr^{642}). AS160 served as a control. (G) L6 cells were transiently transfected with an *AKT2* siRNA for 48 h. Cell lysates were analyzed by Western blot using an antibody against phospho-AS160 (Thr^{642}). AS160 served as a control. (A,B,E) Data are expressed as means ± standard errors of the means (n = 3), and one-way ANOVA followed by Bonferroni post-test were used to compare between multiple groups. n.s; not significant, * $p < 0.05$, ** $p < 0.01$, *** $p < 0.001$ as indicated.

Figure 6. CHI3L1 activates AMPK phosphorylation in primary cultured myoblasts. (A) Myoblasts were stimulated with CHI3L1 for the indicated times. Cell lysates were analyzed by Western blot using antibodies against phospho-AMPKα (Thr^{172}) and phospho-AKT (Ser^{473}). p-AMPKα and p-AKT levels were quantified by densitometry and normalized to total AMPKα and AKT protein levels. Data are expressed as means ± standard errors of the means (n = 3), and one-way ANOVA followed by Bonferroni post-test were used to compare between multiple groups. * $p < 0.05$, ** $p < 0.01$, *** $p < 0.001$ as indicated. (B) For Ca^{2+} detection, myoblasts were preincubated with Fluo-3 AM (5 μM) for 30 min. Ca^{2+} response was measured using a confocal microscope after treatment with CHI3L1. Scale bars, 100 μm. (C) Myoblasts were pretreated with the CaMKK inhibitor STO-609 (5 μM) and then with CHI3L1 (100 ng/mL). Cell lysates were analyzed by Western blot using an antibody against phospho-AMPKα (Thr^{172}). AMPKα served as a control. (D) Myoblasts were pretreated with compound C (30 μM) and then with CHI3L1 (100 ng/mL). Cell lysates were analyzed by Western blot using antibodies against phospho-AS160 (Thr^{642}) and phospho-p38 MAPK. AS160 and p38 MAPK served as controls.

Figure 7. Exercise elevates CHI3L1 expression in skeletal muscle. (A) Total mRNA was prepared from differentiated L6 myotube cells after EPS, and RT-PCR was performed using *CHI3L1*-specific primers. PCR products were separated on 1.7% agarose gels and visualized under ultraviolet light with *ACTB* as a positive control. (B) L6 cells were subjected to several rounds of EPS. Lysates were analyzed by Western blot using an antibody against phospho-AMPKα (Thr^{172}). p-AMPKα levels were quantified by densitometry and normalized to total AMPKα protein levels. Data are expressed as means ± standard errors of the means (n = 3), and one-way ANOVA followed by Bonferroni post-test were used to compare between multiple groups. * $p < 0.05$ as indicated. (C) Mice were sacrificed after exercise and levels of circulating CHI3L1 were measured by ELISA. Data are expressed as means ± standard errors of the means (n = 5 per group), and Student's *t*-test were used to compare between groups. ** $p < 0.01$

as indicated. (D) Muscle tissues from the same animals were lysed for Western blot analysis using an antibody against phospho-AMPKα (Thr^{172}). AMPKα served as a control.

Figure 8. Associations among plasma CHI3L1 levels, *CHI3L1* genetic variants, and lymphocytic *CHI31L* mRNA expression. (A) Plasma CHI3L1 levels of young NGT (n = 20) and old NGT (n = 20). (B) Plasma CHI3L1 levels of old NGT (n = 20) and old IGF+DM (n = 40) groups. (C) Genetic association of *CHI3L1* with risk for DM and diabetic traits. Values are presented as HR or beta coefficient with 95% CI. *P*-values were obtained from Cox proportional hazards regression or multiple linear regression analysis after adjustment for sex, age, area, education level, smoking, drinking, hypertension, and metabolic equivalent. (D) Comparison of relative *CHI3L1* mRNA expression in LCLs (fold change) according to *CHI3L1* genotype, analyzed using Reverse transcription quantitative PCR. (E) Comparison of GLUAUC levels between physically inactive with lower *CHI3L1* mRNA expression and physically active with higher *CHI3L1* mRNA expression. (A,B,D,E) Data are expressed as means ± standard errors of the means, and Student's *t*-test were used to compare between groups. * $p < 0.05$, ** $p < 0.01$, *** $p < 0.001$ as indicated.

Figure 9. A schematic diagram showing the signaling pathways of CHI3L1 involved in glucose metabolism.

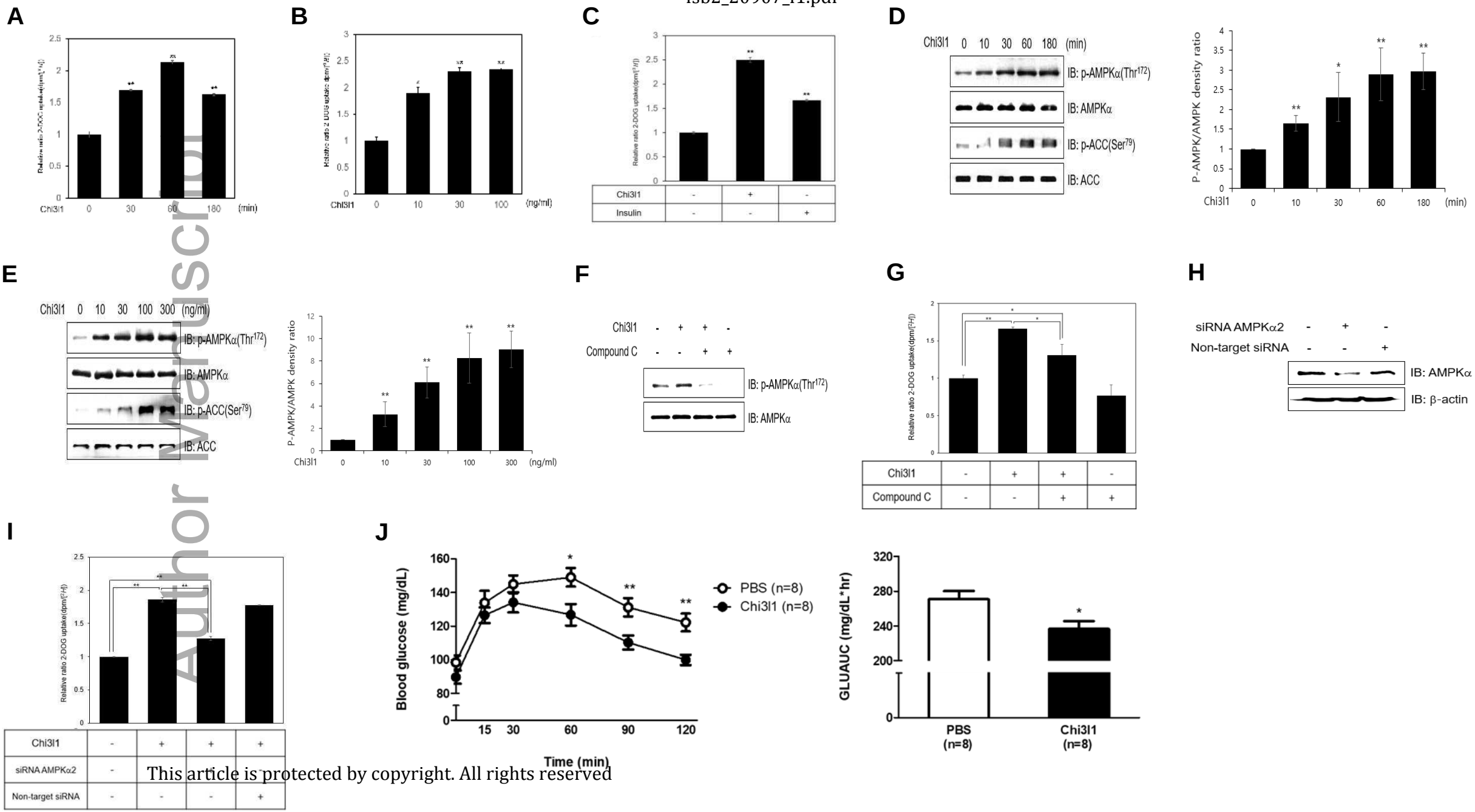

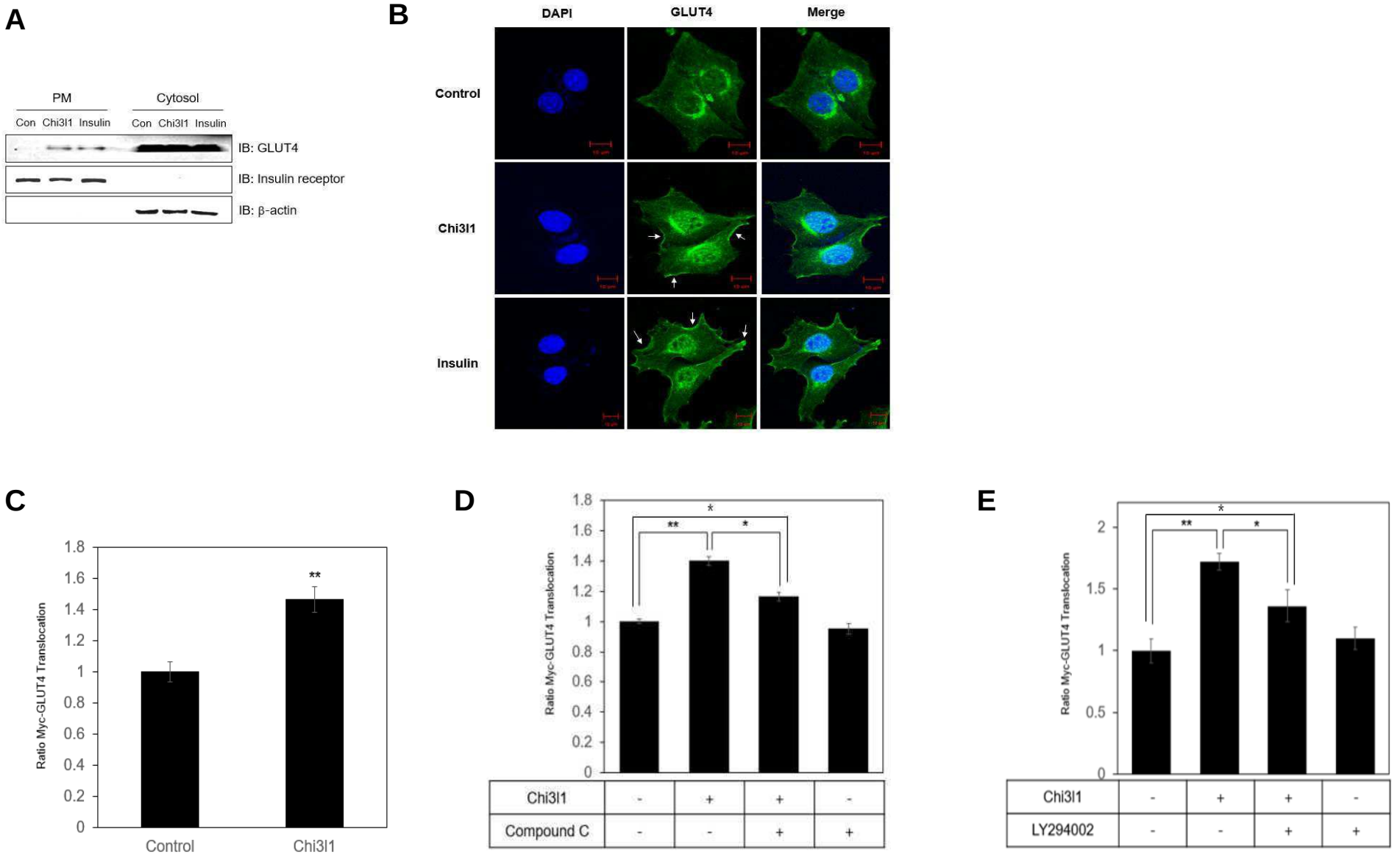

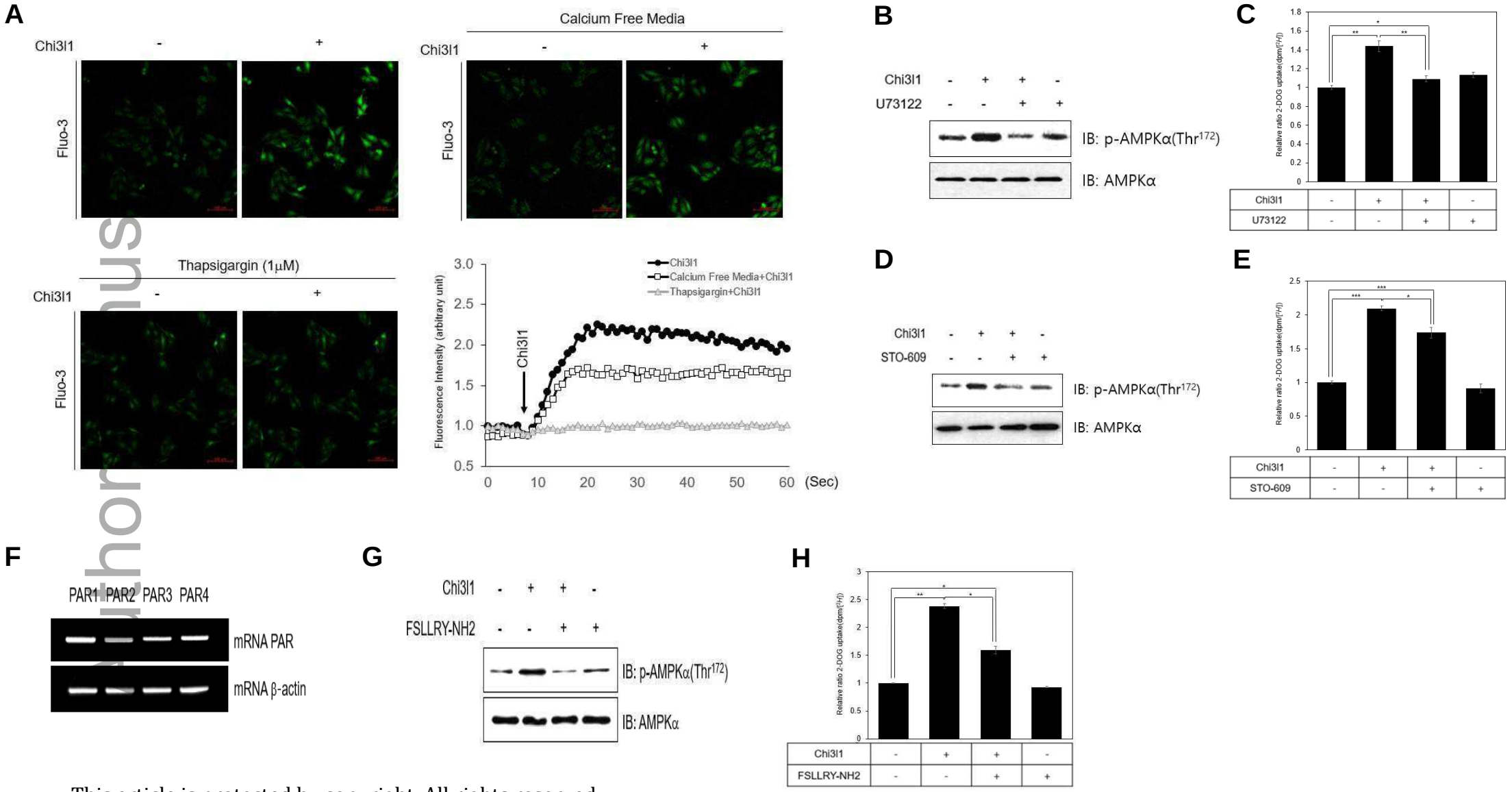

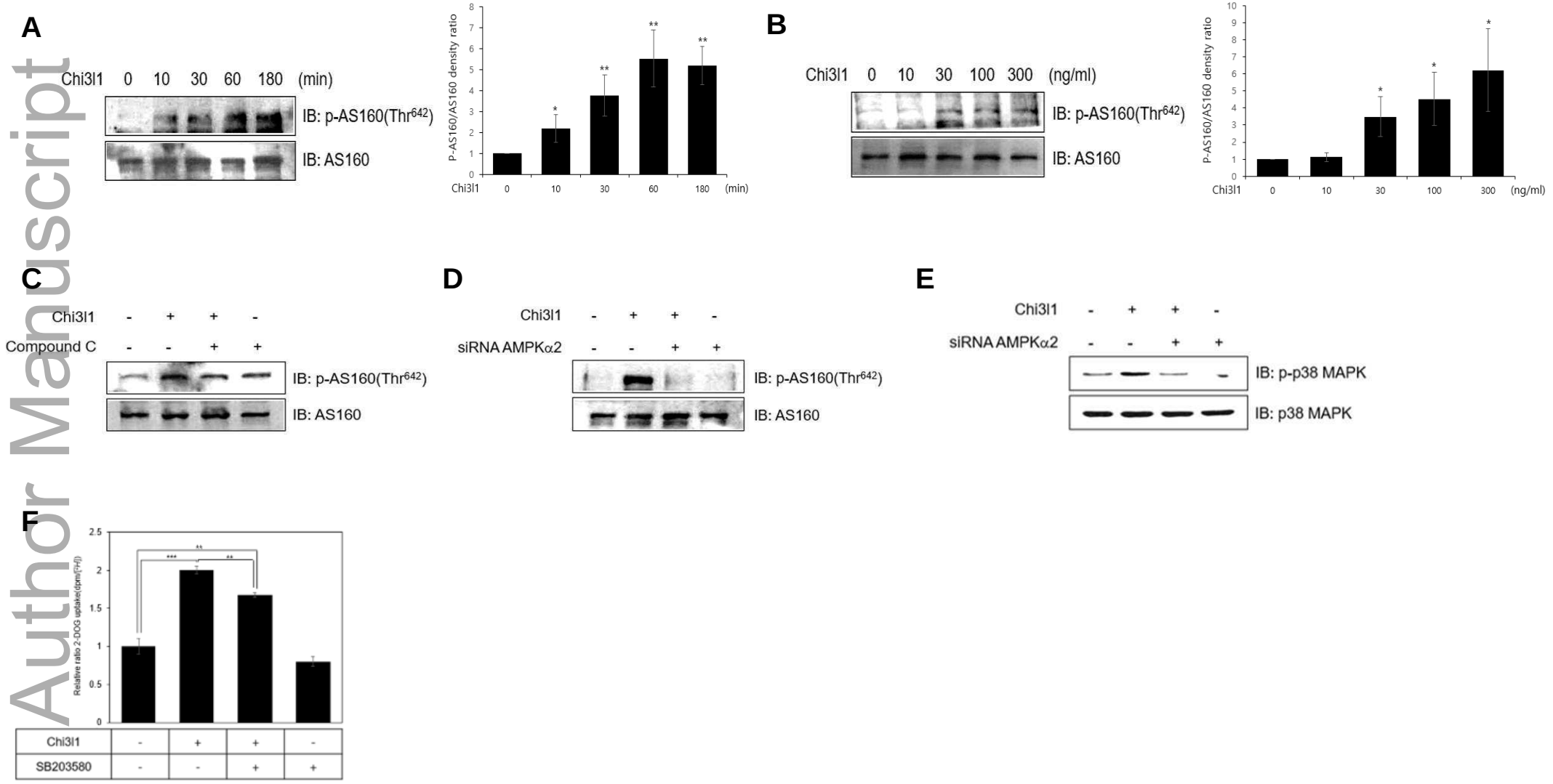

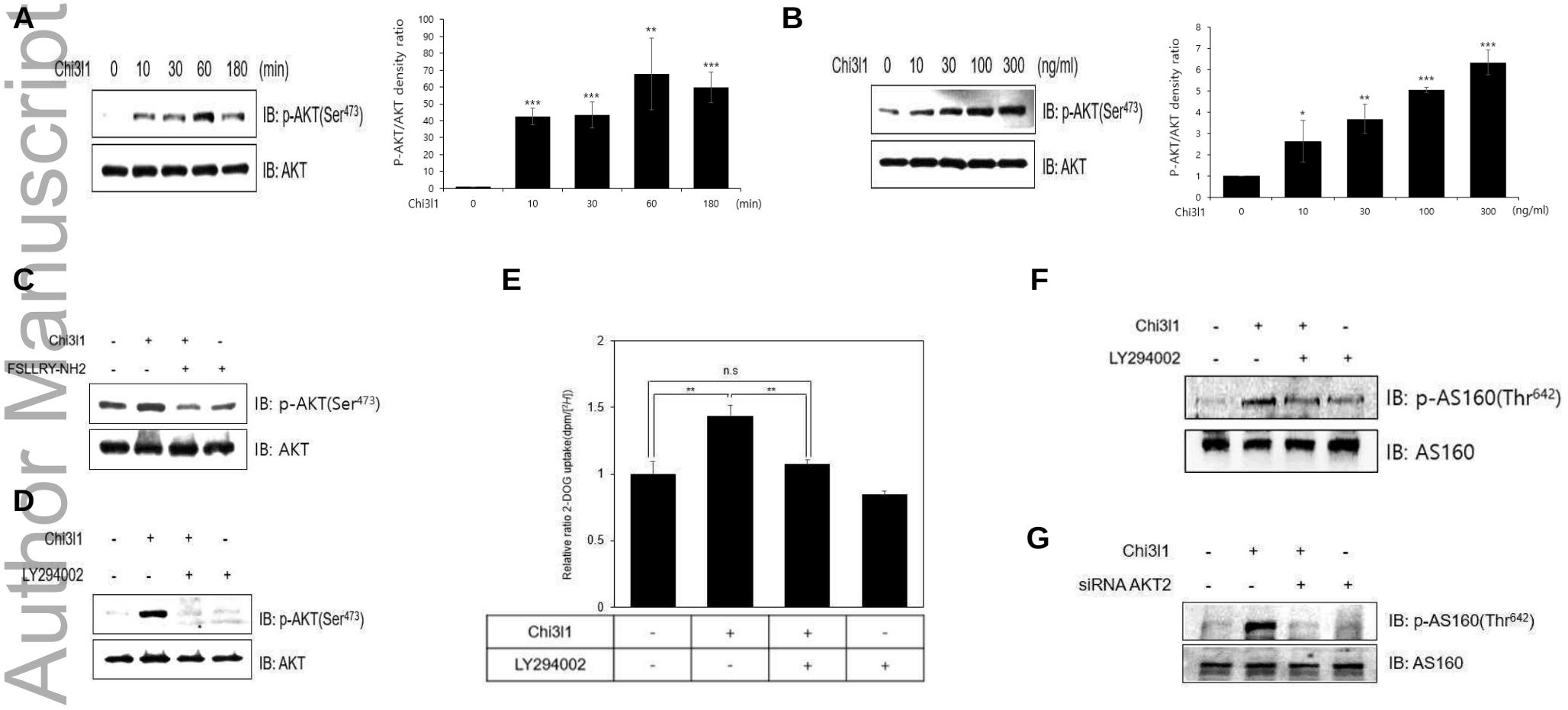

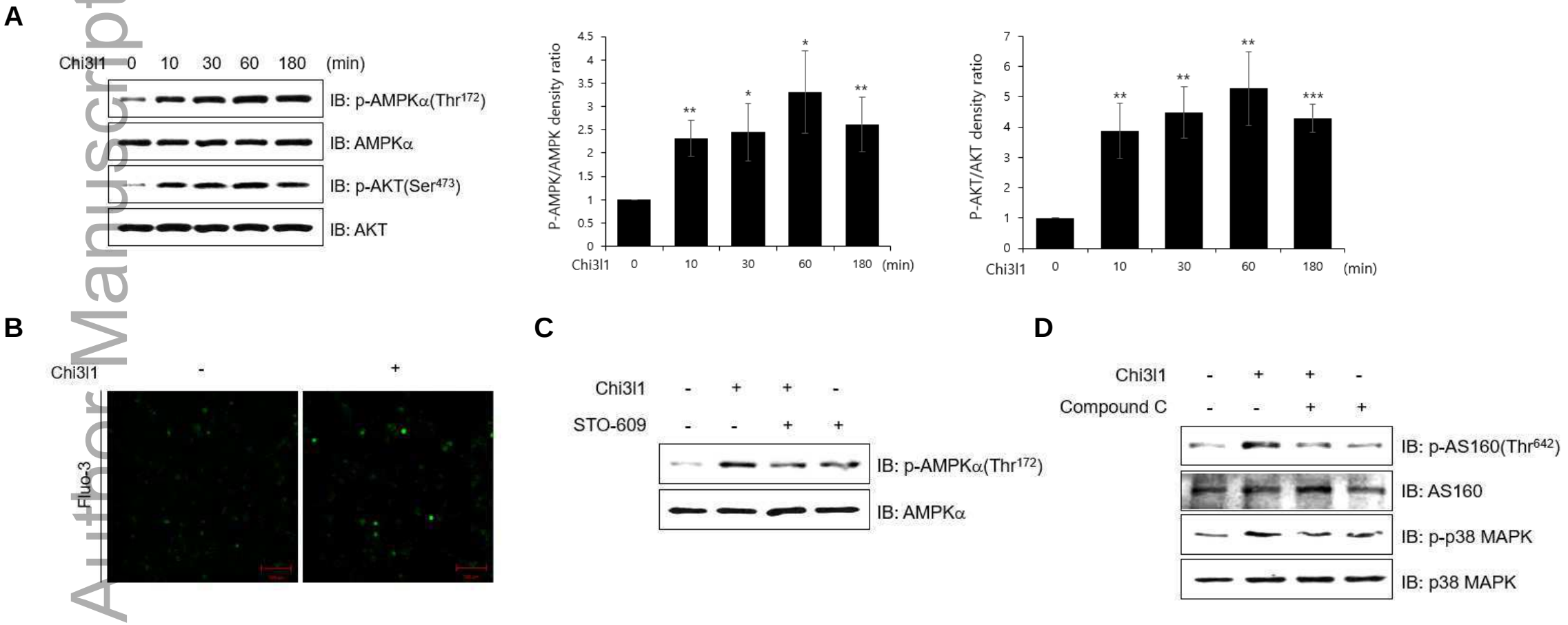

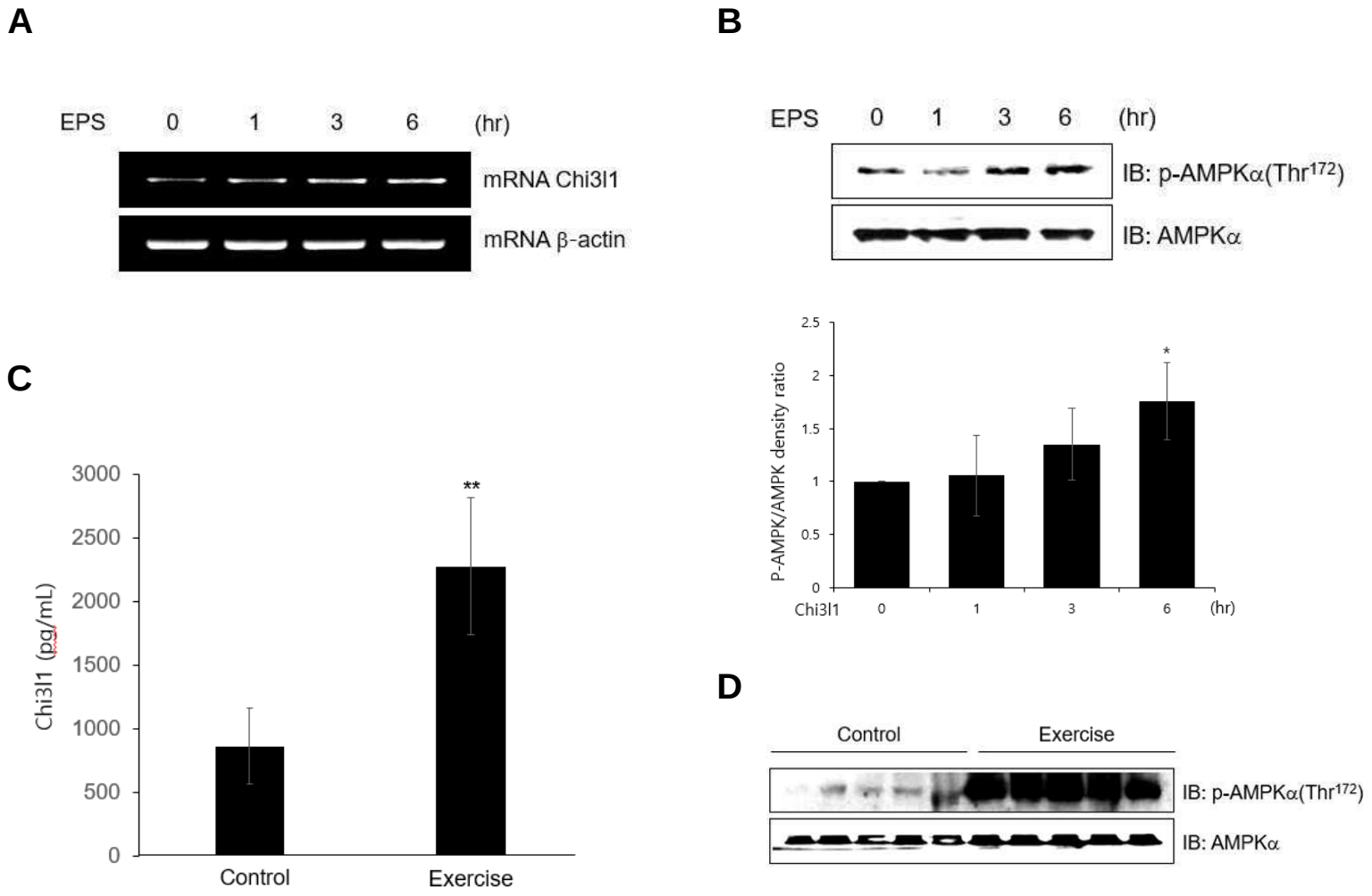

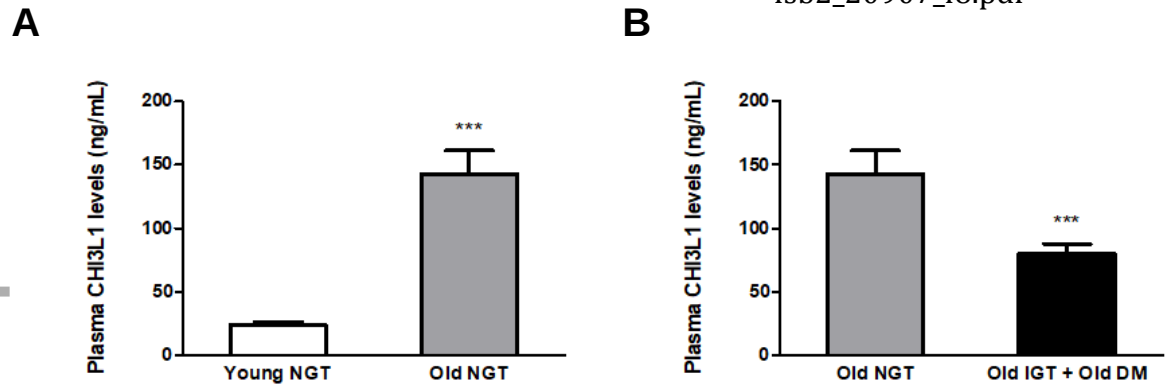

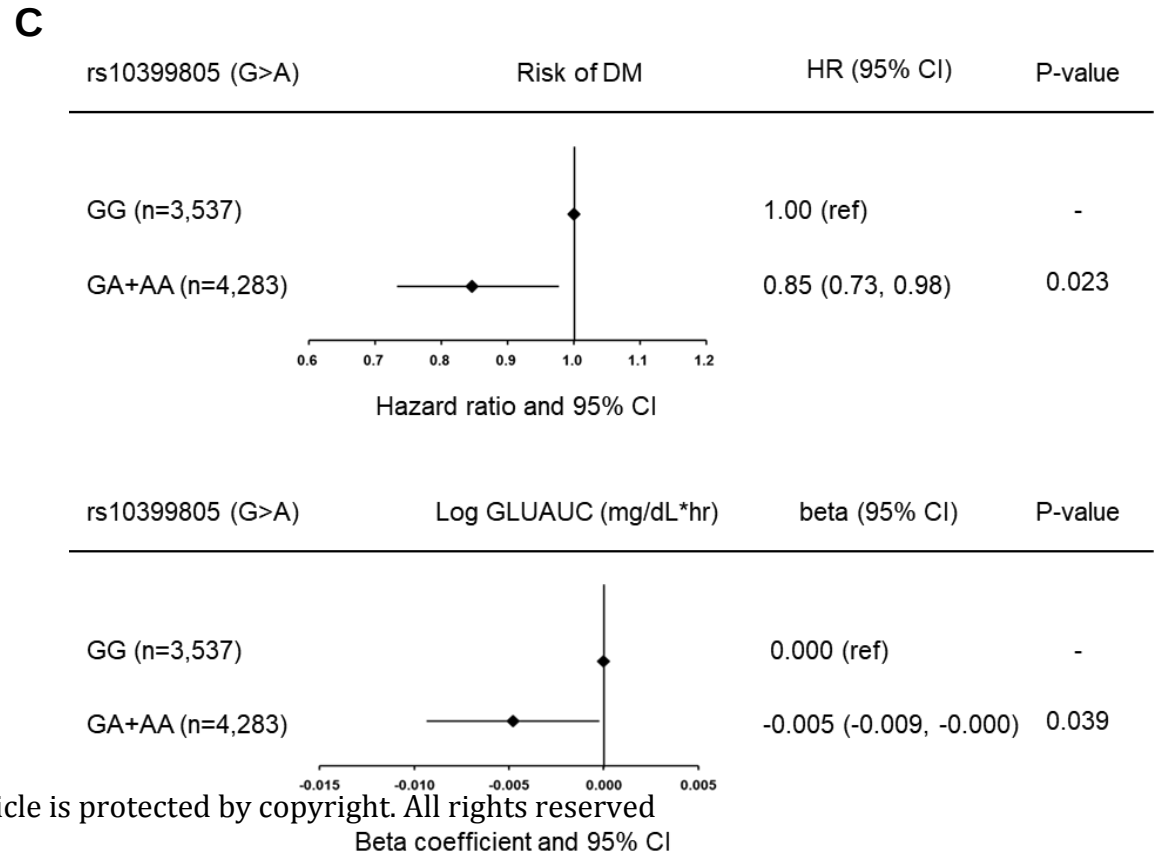

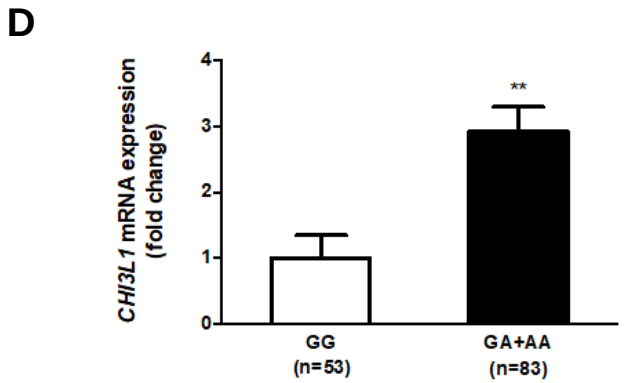

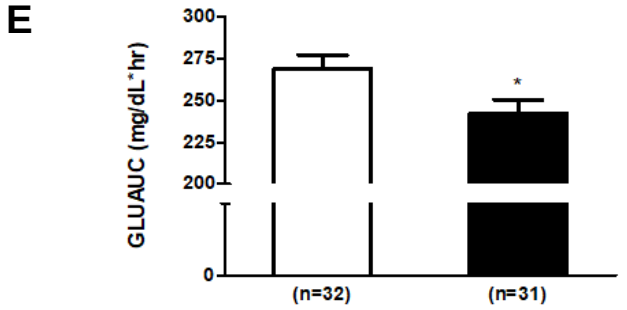

Physical activity	Inactive	Active
CHI3L1 mRNA expression	Low	High

fsb2_20907_f9.pdf